

# Generating Many Majorana Modes via Periodic Driving: A Superconductor Model

Qing-Jun Tong,<sup>1</sup> Jun-Hong An,<sup>1,2,\*</sup> Jiangbin Gong,<sup>3</sup> Hong-Gang Luo,<sup>1,4</sup> and C. H. Oh<sup>2</sup>

<sup>1</sup>Center for Interdisciplinary Studies & Key Laboratory for Magnetism and Magnetic Materials of the MoE, Lanzhou University, Lanzhou 730000, China

<sup>2</sup>Center for Quantum Technologies and Department of Physics, National University of Singapore, 3 Science Drive 2, Singapore 117543, Singapore

<sup>3</sup>Department of Physics and Centre for Computational Science and Engineering, National University of Singapore, Singapore 117542, Singapore

<sup>4</sup>Beijing Computational Science Research Center, Beijing 100084, China

Realizing Majorana modes in condensed-matter systems is of vast experimental and theoretical interests, and some signatures of Majorana modes have been measured already. To facilitate future experimental observations and to explore further applications of Majorana modes, generating *many* Majorana modes at ease in an experimentally accessible manner has become one important issue. This task is achieved here in a one-dimensional  $p$ -wave superconductor system with the nearest- and next-nearest-neighbor interactions. In particular, a periodic modulation of some system parameters can induce an effective long-range interaction (as suggested by the Baker-Campbell-Hausdorff formula) and may recover time-reversal symmetry already broken in undriven cases. By exploiting these two independent mechanisms at once we have established a general method in generating many Floquet Majorana modes via periodic driving.

PACS numbers: 03.67.Lx, 03.65.Vf, 71.10.Pm

*Introduction.*—The Majorana fermion, a particle of its own anti-particle [1], is attracting tremendous attention [2–5]. In addition to its fundamental interest [6–9], its potential applications in topological quantum computation are also noteworthy [10, 11]. Along with considerable theoretical studies [7, 10, 12–20], the experimental search for Majorana modes in condensed-matter systems has become a timely and important research topic. Indeed, following the theoretical results in Refs. [15, 16, 21–25], the zero-bias conductance peaks observed recently [26–29] are regarded as a signature of Majorana modes in one-dimensional (1D) spin-orbit coupled semiconductor nanowires. However, the observed zero-bias peaks can be due to other reasons as well, e.g., the strong disorder in the nanowire [30, 31] or smooth confinement potential at the wire end [32]. This being the case, the formation of Majorana modes in these nanowire systems are yet to be double-confirmed by other approaches.

To facilitate experimental observation of Majorana modes, their signal strength should be enhanced so as to combat against experimental disorder [24, 30, 33] and contaminations from thermal excitations [21–25]. To that end, it is constructive to find a general method to form *many* Majorana modes within one single system [34–36]. This turns out to be a challenging task. One main reason is that the formation of many Majorana modes needs the protection of time-reversal symmetry [36–38], thus imposing a strong restriction. Reference [37] remarked that three or even more pairs of Majorana modes can be obtained by considering a “longer-range” interaction in a system. This is a stimulating suggestion, hinting that the more long-ranged the interaction is, the more Majorana modes one might obtain. Generating many Majorana modes then reduces to the following theoretical

question: how to synthesize a long-range interaction in a topologically nontrivial condensed-matter system while maintaining time-reversal symmetry?

Our answer to the above question is rather straightforward. Given that periodic driving is becoming one highly controllable and versatile tool in generating different topological states of matter [39–44], we advocate to use a periodic driving protocol to induce effective long-range interactions and to restore time-reversal symmetry (if it is broken without driving). Specifically, we switch a Hamiltonian from  $H_1$  for the first half period to  $H_2$  for the second half period. The Floquet operator  $U$ , i.e., the unitary evolution operator associated with each modulation period  $T$ , is then given by

$$U(T) = e^{-\frac{iH_2T}{2\hbar}} e^{-\frac{iH_1T}{2\hbar}} \equiv e^{-\frac{iH_{\text{eff}}T}{\hbar}}, \quad (1)$$

where an effective Hamiltonian  $H_{\text{eff}}$  for the modulated system is also defined. Using the Baker-Campbell-Hausdorff (BCH) formula, one finds that  $H_{\text{eff}}$  defined in Eq. (1) is formally given by

$$H_{\text{eff}} = \frac{H_1}{2} + \frac{H_2}{2} - \frac{iT}{8\hbar} [H_2, H_1] - \frac{T^2}{96\hbar^2} [(H_2 - H_1), [H_2, H_1]] + \cdots \quad (2)$$

Clearly then, even if  $H_1$  or  $H_2$  are short-range Hamiltonians, the engineered  $H_{\text{eff}}$  may still have long-range hopping or pairing terms via the nested-commutator terms [see Eq. (2)]. Thus, the remaining job is to design such a protocol so that  $H_{\text{eff}}$  also possesses time-reversal symmetry. Interestingly, in the first proposal to realize Floquet Majorana modes [44], no more than two pairs of Majorana modes can be generated precisely because time-

reversal symmetry is not restored by the periodic driving therein.

In the following we present our detailed results using a model of a 1D spinless  $p$ -wave superconductor with the nearest- and next-nearest-neighbor (NNN) interactions only. The introduction of the NNN interaction will facilitate us to have time-reversal-symmetry preserved and broken cases and thus to realize their conversion by our proposed driven protocol. Under open boundary condition and under a periodic modulation of superconducting phase parameters, we not only demonstrate that many Floquet Majorana modes (e.g., 13 pairs in one case) can be generated, but also show that the exact number of the Majorana modes may be widely tuned by scanning the modulation period. These results also shed more light on the inherent advantages of driven systems in synthesizing Majorana modes.

*Static model.*—We start from the Kitaev model Hamiltonian for a 1D spinless  $p$ -wave superconductor

$$H = -\mu \sum_{l=1}^N c_l^\dagger c_l - \sum_{l=1}^{N-1} (t_1 c_l^\dagger c_{l+1} + \Delta_1 c_l^\dagger c_{l+1}^\dagger + \text{h.c.}) - \sum_{l=1}^{N-2} (t_2 c_l^\dagger c_{l+2} + \Delta_2 c_l^\dagger c_{l+2}^\dagger + \text{h.c.}), \quad (3)$$

where  $\mu$  is the chemical potential,  $t_a$  and  $\Delta_a = |\Delta_a| e^{i\phi_a}$  with  $a = 1$  ( $a = 2$ ) describe the nearest- (next-nearest-) neighbor hopping amplitude and pairing potential respectively, and  $\phi_a$  is the associated superconducting phases. All energy-related parameters are scaled by  $|\Delta_1|$  and hence dimensionless. For convenience we set  $\hbar = 1$  in our detailed calculations. Majorana operators here refer to  $(c_l + c_l^\dagger)$  or  $i(c_l - c_l^\dagger)$ . Such synthesized Majorana modes may appear as edge modes under open boundary condition, if the bulk band structure is topologically nontrivial.

The relative phase  $\phi = \phi_1 - \phi_2$  determines the topological class of  $H$  [45]. For  $\phi = 0$  and  $\pi$ ,  $H$  has time-reversal and particle-hole symmetries. These cases then belong to the so-called “BDI” class characterized by a topological invariant  $Z$ . For other values of  $\phi$ ,  $H$  has particle-hole symmetry only and falls into the so-called “D” class characterized by a topological invariant  $Z_2$ . The D class can generate at most one pair of Majorana modes. As to the BDI class, despite its potential in forming many Majorana modes [38], at most two pairs of Majorana modes can be generated here due to the short-range nature of  $H$ .

*Driven model.*—We now turn to periodically driven cases under a driving protocol given by Eq. (1). The emergence of Floquet Majorana modes is directly connected with topological properties of the eigenstates of the Floquet operator  $U(T)$ . Let  $|u\rangle$  be an eigenstate of  $U(T)$  with an eigenvalue  $e^{-i\epsilon T}$ , namely  $U(T)|u\rangle = e^{-i\epsilon T}|u\rangle$ . Evidently, this eigenvalue index  $\epsilon$  is defined

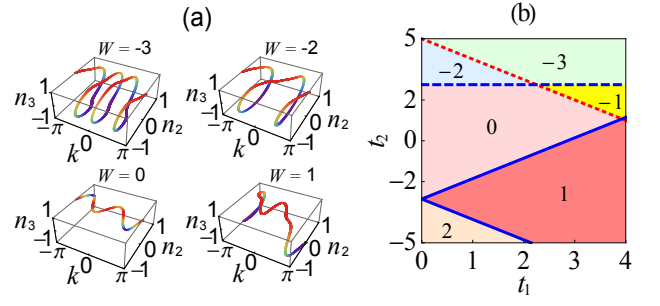


FIG. 1: (Color online) (a) Winding of the unit vector  $\vec{n}(k)$  [see Eqs. (5) and (6)] as  $k$  varies from  $-\pi$  to  $\pi$ , in different parameter regimes under our driving protocol.  $t_1 = 1$ ;  $t_2 = 5$  for  $W = -3$ ,  $t_2 = 3$  for  $W = -2$ ,  $t_2 = 0$  for  $W = 0$ , and  $t_2 = -3$  for  $W = 1$ . (b) Topological phase diagram of our driven system plotted in the  $(t_1, t_2)$  plane. Indicated on each regime is the winding number  $W$ , which gives the number of pairs of Majorana modes. The solid and dotted line indicates a gap closing (of  $E_k$ ) at  $k = 0$  or  $\pm\pi$ , while the dashed line corresponds to a gap closing at  $k = \pi/2$ . Other parameters are  $\mu = -10$ ,  $|\Delta_2| = 2.5$  and  $T = 0.2$ .

only up to a period  $2\pi/T$  and hence called “quasi-energy”. The periodicity in  $\epsilon$  may lead to a novel topological structure in driven systems, with the corresponding topological classification revealed by the homotopy groups [42]. However, if the driven system belongs to a trivial class associated with this novel topological structure, then topological properties of the driven system is fully characterized by  $H_{\text{eff}}$  defined in Eq. (1) [38]. This will be the case for our driving protocol proposed below.

Specifically, we switch between the two Hamiltonians  $H_1$  and  $H_2$  by the following: in the first half period,  $H_1 = H(\phi_1, \phi_2)$  with both superconducting phase parameters  $\phi_1$  and  $\phi_2$  fixed; whereas in the second half period, we swap  $\phi_1$  and  $\phi_2$  so that  $H_2 = H(\phi_2, \phi_1)$ . Without loss of generality we choose  $\phi = \phi_1 - \phi_2 = \pm\pi/2$ . Thus, within each half period, the Hamiltonian is in class D that breaks time-reversal symmetry. In addition to a possible generation of long-range interactions for  $H_{\text{eff}}$ , this driving protocol is designed to recover time-reversal symmetry. In particular, let  $\mathcal{K}$  be a conventional time-reversal operator and  $G \equiv e^{-i\frac{\phi_1+\phi_2}{2}\sum_l c_l^\dagger c_l}$  be a gauge transformation operator. Considering a generalized time-reversal operator  $\bar{\mathcal{K}} \equiv \mathcal{K}G$ , we find

$$\bar{\mathcal{K}}U(T)\bar{\mathcal{K}}^{-1} = e^{\frac{iH_1T}{2\hbar}}e^{\frac{iH_2T}{2\hbar}} = U^\dagger(T). \quad (4)$$

This constitutes a direct proof that our driven system now possesses time-reversal symmetry, and as a result its topological class is switched from class D to class BDI. To further examine this restored time-reversal symmetry, we work in the momentum representation and directly find an analytical  $H_{\text{eff}}$  from Eq. (1). We define  $c_k = \sum_l c_l e^{-ikl}/\sqrt{N}$  and introduce the particle-

hole representation  $C_k = [c_k, c_{-k}^\dagger]^T$ . A standard procedure then leads to  $H_{\text{eff}} = \sum_{k \in \text{BZ}} C_k^\dagger H_{\text{eff}}(k) C_k$ , with  $H_{\text{eff}}(k) = E_k \vec{n}(k) \cdot \vec{\sigma}$ , where  $\vec{\sigma}$  represents the Pauli matrices [41]. The three components of  $\vec{n}(k)$  are given by  $n_1(k) = 0$ , and

$$n_2(k) = \frac{g_{1,k} \sin(s_k T)}{s_k \sin(E_k T)} - \frac{2g_{2,k} \eta_k \sin^2 s_k T/2}{s_k^2 \sin(E_k T)}, \quad (5)$$

$$n_3(k) = \frac{\eta_k \sin(s_k T)}{s_k \sin(E_k T)} + \frac{2g_{1,k} g_{2,k} \sin^2 s_k T/2}{s_k^2 \sin(E_k T)}, \quad (6)$$

where  $g_{a,k} = |\Delta_a| \sin(ak)$ ,  $s_k = (\eta_k^2 + \sum_a g_{a,k}^2)^{1/2}$ ,  $\eta_k = -\mu - 2 \sum_a t_a \cos(ak)$ , and  $\cos(E_k T) = \cos(s_k T) + 2(g_{2,k}^2/s_k^2) \sin^2 s_k T/2$ . For each value of  $k$ , one obtains two values of  $E_k$  and hence two values for the quasi-energy  $\epsilon$ . Consistent with the  $\tilde{K}$  symmetry, we now have  $H_{\text{eff}}^*(-k) = H_{\text{eff}}(k)$ . Noting the inherent particle-hole symmetry of  $H_{\text{eff}}$ , one may construct a chiral symmetry for  $H_{\text{eff}}$ , a fact consistent with our above result that  $\vec{n}(k)$  is in the  $yz$  plane for all  $k$ . The above analysis makes it clear that our driving protocol changes both the underlying symmetry and the topological class of the system.

Without a gap closing between the two branches of  $E_k$ , the topological invariant  $Z$  in class BDI can be obtained by the integer winding number  $W = \int_{-\pi}^{\pi} \frac{d\theta_k}{2\pi} \in \mathbb{Z}$ , where  $\theta_k = \arctan[n_3(k)/n_2(k)]$ . Geometrically,  $W$  means the number of times the vector  $\vec{n}(k)$  rotates around the origin point as  $k$  varies from  $-\pi$  to  $\pi$ . An example is shown in Fig. 1(a). The number of pairs of Majorana modes under open boundary condition is then given by  $|W|$ . As some system parameters continuously change, gap closing and consequently topological phase transitions occur [7]. Figure 1(b) depicts a phase diagram, obtained by explicitly evaluating  $W$ . It is seen that  $|W|$  ranges from 0 to 3. This indicates that three pairs of Majorana modes can be formed in our driven system. This is beyond the expectation for the undriven model, where the NNN interaction can give at most two pairs of Majorana modes. Therefore, the finding of  $|W| = 3$  in some parameter regime is the first clear sign that our driving protocol may synthesize some features absent in the static model. The boundaries between different topological phases of our driven system, as presented in Fig. 1(b) by the solid, dashed, and dotted lines, are also interesting on their own right. For example, the solid and dotted lines depict the topological phase transition points at which  $W$  jumps by one. This is found to go with the gap closing at  $k = 0$  or  $\pm\pi$ . Noting that  $n_2(k) = 0$  for  $k = 0$  or  $\pm\pi$ , the solid and dotted lines are found to satisfy  $\sin[(\pm 2t_1 - 2t_2 - \mu)T] = 0$ , which gives  $n_3(k) = 0$  for  $k = 0$  or  $\pm\pi$ . On the other hand, the dashed line in Fig. 1(b) gives the phase transition points at which  $W$  jumps by two. This happens at  $k = \pi/2$  and the critical  $t_2$  values satisfy  $t_2 = (\mu + \sqrt{(\pi/T)^2 - |\Delta_1|^2})/2$ , for which  $n_2(k) = n_3(k) = 0$  for  $k = \pi/2$ . Such a phase border line is independent of  $t_1$  and  $|\Delta_2|$ , thus explaining why the

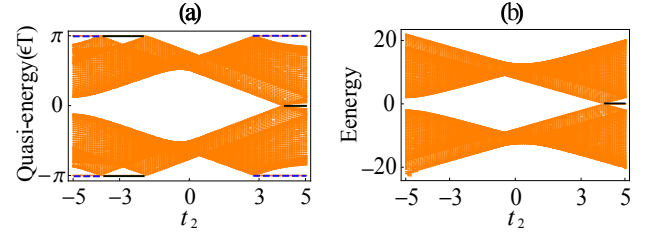


FIG. 2: (Color online) Comparison between quasi-energy spectrum for the driven case (a) and energy spectrum for the static case (b), both numerically obtained under open boundary condition. The dashed (blue) line in (a) stands for two degenerate pairs of Majorana modes, and the solid (black) lines in (a) and (b) stand for a single pair. The results agree with the topological phase diagram in Fig. 1(b). Here  $t_1 = 1$ ,  $N = 200$ , and other parameters are the same as in Fig. 1(b).

dashed line in Fig. 1(b) is horizontal.

To confirm our theoretical results presented in Fig. 1 we carry out numerical calculations of the quasi-energy spectrum  $\epsilon$  under open boundary condition. Because  $\epsilon = \pi/T$  is equivalent to  $\epsilon = -\pi/T$ , Floquet Majorana modes have two flavors: one at  $\epsilon = 0$  and the other at  $\epsilon = \pm\pi/T$ . The second flavor is certainly absent in an undriven system [44]. For fixed  $t_1 = 1$  and a varying  $t_2$ , Fig. 2(a) depicts the formation of both flavors of Floquet Majorana modes obtained numerically, with the second flavor emerging in a wider parameter regime. The total number of pairs of Majorana modes should equal  $|W|$  (if the winding number is well defined). As an example, consider the case with  $t_1 = 1$  and  $t_2 = 4$ . Figure 2(a) shows the formation of two degenerate pairs of Majorana modes at  $\epsilon = \pm\pi/T$  and one pair of Majorana mode at  $\epsilon = 0$ . This agrees with the  $W = -3$  region shown in Fig. 1(b). Likewise, all other details shown in Fig. 2(a) are fully consistent with our analytical results shown in Fig. 1(b). We have also studied the dynamics of the formed Majorana modes in one full period of driving: they are indeed well localized at two edges. Further, as a comparison with our static model  $H$ , we plot in Fig. 2(b) our system's energy spectrum in the absence of driving. It is seen that at most one pair of Majorana modes can be formed. Indeed, theoretical analysis for the undriven case in the class D yields that the associated  $Z_2$  topological number is given by  $\nu = \text{sgn}[(2t_2 + \mu)^2 - 4t_1]$  and at most one pair of Majorana modes may be formed when  $\nu = -1$ . For a negative  $\mu$  but with large  $|\mu|$ , one has  $\nu = -1$  only in a very narrow parameter regime. The parallel driven case with a large large  $|\mu|$  is however different: one may still obtain three pairs of Majorana modes. Thus, even in regimes of large  $|\mu|$ , our driving protocol can still generate more Majorana modes than the static case. This is both interesting and useful because in general, the regime of large  $|\mu|$  is preferred for the protection of Majorana modes against

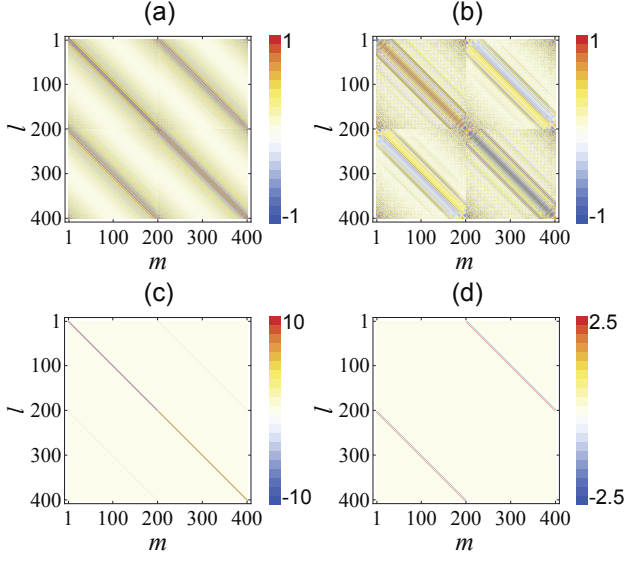


FIG. 3: (Color online) The expansion coefficients of  $H_{\text{eff}}$  for  $T = 0.2$  (a) and  $T = 2.0$  (b), and of the static  $H$  for the real (c) and imaginary (d) parts, when  $H_{\text{eff}}$  or  $H$  are expanded as a quadratic function of the operators  $(c_1, \dots, c_N, c_1^\dagger, \dots, c_N^\dagger)$ , with  $N = 200$ , and  $l$  and  $m$  being the operator base indices ranging from 1 to 400. Other system parameters are the same as in Fig. 2.

strong disorder in actual experiments.

In efforts to generate even more Majorana modes, we now extend our direct numerical studies to other parameter regimes. Remarkably, the BCH formula in Eq. (2) indicates that as  $T$  increases, the nested commutators on the right hand side of Eq. (2) will have heavier weights. An increasing  $T$  can then induce longer-range interactions in  $H_{\text{eff}}$ . This trend is investigated in Fig. 3, where the expansion coefficients of  $H_{\text{eff}}$  [numerically obtained from Eq. (1)], with  $H_{\text{eff}}$  expanded as a quadratic function of the operators  $(c_1, \dots, c_N, c_1^\dagger, \dots, c_N^\dagger)^T$ , are shown for two different values of  $T$ . For comparison, the expansion coefficients for the static case are also plotted in Fig. 3(c,d). A few interesting observations can be made from Fig. 3. First, the plotted expansion coefficients of  $H_{\text{eff}}$  are all real, which is different from the shown static case with both real and imaginary coefficients. This difference reflects the restored time-reversal symmetry for the driven case. Second, in sharp contrast to the results shown in Fig. 3(c,d), coefficients for quite long-range hopping/pairing (e.g., across more than 10 sites) can be appreciably nonzero for  $H_{\text{eff}}$  in both cases of  $T = 0.2$  and  $T = 2.0$ . The latter case, plotted in Fig. 3(b) with wider stripes, confirms the emergence of longer-range terms with considerable weights as  $T$  increases. Third, the diagonal terms in the expansion shown in Fig. 3(a,b) (which can be understood as an effective chemical potential) are much smaller than the diagonal elements, i.e.

$|\mu|$ , in Fig. 3(c). This further explains why a driven system may generate many Majorana modes despite a large  $|\mu|$  in the undriven model.

Results in Fig. 3 motivate us to explore the formation of Floquet Majorana modes with sufficiently large values of  $T$ . There is also one twist as we increase  $T$ . That is, the quasi-energy gap may be generically closed at  $\epsilon = 0$  but still open at  $\epsilon = \pm\pi/T$ . Consequently the winding number  $W$  is no longer well-defined and one is forced to count the formed pairs of Majorana modes, one by one, at  $\epsilon = \pm\pi/T$ . We indeed do this and present in Tab. I the number of pairs of Majorana modes we obtain, for an increasing  $T$  and for different choices of  $t_2$ . For  $T = 0.5$ , the best observation is the generation of 4 pairs of Majorana modes. For  $T = 1.0$ , it is possible to achieve 7 pairs. For  $T = 2.0$ , as many as 13 pairs of Majorana modes can be formed. Interestingly, as indicated in Tab. I, for large values of  $T$  such as  $T = 1.0$  and  $T = 2.0$ , our driving protocol can also form several pairs of Majorana modes with  $t_2 = 0$ . Note also that as more Majorana modes are generated by increasing  $T$ , the bulk quasi-energy gap at  $\epsilon = \pm\pi/T$  decreases in general, leading to a larger “penetration length” (into the bulk) for the synthesized Majorana modes. Considering the necessary protection of Majorana modes by a nonzero bulk gap, one may not wish to push our driving protocol too far.

TABLE I: Number of Majorana modes localized at each boundary for different values of  $T$ . Other parameters are the same as in Fig. 2(a). The parentheses indicate that the system is in a close neighborhood of a topological phase transition.

$t_2$	-8	-7	-6	-5	-4	-3	-2	-1	0	1	2	3	4	5	6	7	8
$T = 0.5$	(2)	4	4	3	3	2	(0)	0	0	1	1	2	2	4	4	4	3
$T = 1.0$	6	(6)	7	(7)	6	3	3	2	1	1	2	5	5	6	7	7	6
$T = 2.0$	13	13	12	11	9	8	8	1	1	3	(4)	7	11	10	13	13	12

*Conclusions.*—A periodic driving has the capacity to restore time-reversal symmetry and to induce an effective long-range interaction. With these two mechanisms working at once, the generation of many Majorana modes is achieved using a standard  $p$ -wave superconductor model under certain periodic modulation.

In terms of possible experimental confirmation of our predictions, our model may be realized with cold atoms or molecules in a designed optical lattice. Explicitly, the nearest and NNN hopping ( $t_a$ ) can be realized by a simple zigzag chain lattice [35], with the hopping strength adjustable by the lattice geometry. The chemical potential ( $\mu$ ) is controllable through the optical trap potential or a radio frequency detuning. The pairing terms ( $\Delta_a$ ) may be induced by a Raman induced dissociation of Cooper pairs forming an atomic BCS reservoir and the associated superconducting phases ( $\phi_a$ ) can be tuned by com-



plex Rabi frequencies [44]. An alternative experimental realization is to use the recently proposed quantum-dot-superconductor arrays with a zigzag geometry [46]. Here the chemical potential can be gate controlled. The pairing potentials can be proximity-induced and their phases can be tuned via applying fluxes on the superconducting islands. The Majorana modes formed in our system may be probed using techniques analogous to what is being used for undriven systems [35], but now with the hope of some enhanced signals if a measurement exploits the simultaneous generation of *many* Majorana modes.

*Acknowledgements.*—This work is supported by the Fundamental Research Funds for the Central Universities, by the NSF of China (Grant Nos. 11175072, 11174115, and 10934008), and by National Research Foundation and Ministry of Education, Singapore (Grant No. WBS: R-710-000-008-271). J.G. was funded by Academic Research Fund Tier I, Ministry of Education, Singapore (grant No. R-144-000-276-112).

---

\* Electronic address: [anjhong@lzu.edu.cn](mailto:anjhong@lzu.edu.cn)

- [1] E. Majorana, *Nuovo Cimento*, **5**, 171 (1937).
- [2] C. Nayak, S. H. Simon, A. Stern, M. Freedman, and S. Das Sarma, *Rev. Mod. Phys.* **80**, 1083 (2008).
- [3] F. Wilczek, *Nature Phys.* **5**, 614 (2009).
- [4] C. W. J. Beenakker, arXiv:1112.1950.
- [5] J. Alicea, *Rep. Prog. Phys.* **75**, 076501 (2012).
- [6] G. Moore and N. Read, *Nucl. Phys. B* **360**, 362 (1991).
- [7] N. Read and D. Green, *Phys. Rev. B* **61**, 10267 (2000).
- [8] D. A. Ivanov, *Phys. Rev. Lett.* **86**, 268 (2001);
- [9] J. Alicea, Y. Oreg, G. Refael, F. von Oppen, and M. P. A. Fisher, *Nature Phys.* **7**, 412 (2011).
- [10] A. Kitaev, *Phys. Usp.* **44**, 131 (2001).
- [11] A. Kitaev, *Ann. Phys.* **303**, 2 (2003); **321**, 2 (2006).
- [12] L. Fu and C. L. Kane, *Phys. Rev. Lett.* **100**, 096407 (2008); *Phys. Rev. B*, **79**, 161408(R) (2009).
- [13] J. D. Sau, R. M. Lutchyn, S. Tewari, and S. Das Sarma, *Phys. Rev. Lett.* **104**, 040502 (2010).
- [14] J. Alicea, *Phys. Rev. B* **81**, 125318 (2010).
- [15] R. M. Lutchyn, J. D. Sau, and S. Das Sarma, *Phys. Rev. Lett.* **105**, 077001 (2010);
- [16] Y. Oreg, G. Refael, and F. von Oppen, *Phys. Rev. Lett.* **105**, 177002 (2010).
- [17] C. Zhang, S. Tewari, R. M. Lutchyn, and S. Das Sarma, *Phys. Rev. Lett.* **101**, 160401 (2008).
- [18] M. Sato, Y. Takahashi, and S. Fujimoto, *Phys. Rev. Lett.* **103**, 020401 (2009).
- [19] S.-L. Zhu, L.-B. Shao, Z. D. Wang, and L.-M. Duan, *Phys. Rev. Lett.* **106**, 100404 (2011).
- [20] M. Gong, G. Chen, S. Jia, C. Zhang, *Phys. Rev. Lett.* **109**, 105302 (2012).
- [21] K. Sengupta, I. Zutic, H.-J. Kwon, V. M. Yakovenko, and S. Das Sarma, *Phys. Rev. B* **63**, 144531 (2001).
- [22] K. T. Law, P. A. Lee, and T. K. Ng, *Phys. Rev. Lett.* **103**, 237001 (2009).
- [23] J. D. Sau, S. Tewari, R. M. Lutchyn, T. D. Stanescu, and S. Das Sarma, *Phys. Rev. B* **82**, 214509 (2010).
- [24] K. Flensberg, *Phys. Rev. B* **82**, 180516 (2010).
- [25] M. Wimmer, A. R. Akhmerov, J. P. Dahlhaus, and C. W. J. Beenakker, *New J. Phys.* **13**, 053016 (2011).
- [26] V. Mourik, K. Zuo, S. M. Frolov, S. R. Plissard, E. P. A. M. Bakkers and L. P. Kouwenhoven, *Science* **336**, 1003 (2012);
- [27] J. R. Williams, A. J. Bestwick, P. Gallagher, S. S. Hong, Y. Cui, A. S. Bleich, J. G. Analytis, I. R. Fisher and D. Goldhaber-Gordon, *Phys. Rev. Lett.* **109**, 056803 (2012).
- [28] M. T. Deng, C. L. Yu, G. Y. Huang, M. Larsson, P. Caroff and H. Q. Xu, arXiv:1204.4130.
- [29] A. Das, Y. Ronen, Y. Most, Y. Oreg, M. Heiblum, and H. Shtrikman, arxiv:1205.7073.
- [30] J. Liu, A. C. Potter, K. T. Law, and P. A. Lee, arXiv:1206.1276.
- [31] D. I. Pikulin, J. P. Dahlhaus, M. Wimmer, and C. W. J. Beenakker, arXiv:1206.6687.
- [32] G. Kells, D. Meidan, and P. W. Brouwer, arXiv:1207.3067.
- [33] V. Shivamoggi, G. Refael, and J. E. Moore, *Phys. Rev. B* **82**, 041405 (2010).
- [34] I. C. Fulga, F. Hassler, A. R. Akhmerov and C. W. J. Beenakker, *Phys. Rev. B* **83**, 155429, (2011).
- [35] C. V. Kraus, S. Diehl, P. Zoller, and M. A. Baranov, arXiv:1201.3253.
- [36] L. Wong and K. Law, arXiv:1110.4575.
- [37] Y. Niu, S. B. Chung, C.-H. Hsu, I. Mandal, S. Raghu, and S. Chakravarty, *Phys Rev B* **85**, 035110 (2012).
- [38] A. P. Schnyder, S. Ryu, A. Furusaki, and A. W. W. Ludwig, *Phys. Rev. B* **78**, 195125 (2008); A. Kitaev, arXiv:0901.2686.
- [39] T. Oka and H. Aoki, *Phys. Rev. B* **79**, 081406 (2009).
- [40] J.-i. Inoue and A. Tanaka, *Phys. Rev. Lett.* **105**, 017401 (2010).
- [41] T. Kitagawa, M. S. Rudner, E. Berg, and E. Demler, *Phys. Rev. A* **82**, 033429 (2010).
- [42] T. Kitagawa, E. Berg, M. Rudner, and E. Demler, *Phys. Rev. B* **82**, 235114 (2010).
- [43] N. H. Lindner, G. Refael, and V. Galitski, *Nature Phys.* **7**, 490 (2011).
- [44] L. Jiang, T. Kitagawa, J. Alicea, A. R. Akhmerov, D. Pekker, G. Refael, J. I. Cirac, E. Demler, M.D. Lukin, and P. Zoller, *Phys. Rev. Lett.* **106**, 220402 (2011).
- [45] S. Ryu, A. P. Schnyder, A. Furusaki, and A. W. W. Ludwig, *New J. Phys.* **12**, 065010 (2010).
- [46] J. D. Sau and S. Das Sarma, *Nat. Commun.* **3**, 964 (2012).